Available online at www.sciencedirect.com
ScienceDirect
Journal of Molecular Catalysis A: Chemical 281 (2008) 146–153
JOURNAL OF MOLECULAR CATALYSIS A: CHEMICAL
www.elsevier.com/locate/molcata

HMS mesoporous silica as cobalt support for the Fischer–Tropsch Synthesis: Pretreatment, cobalt loading and particle size effects

Estephanía Lira [a], Carmen M. López [a], Freddy Oropeza [a], Mónica Bartolini [a], Juan Alvarez [a], Mireya Goldwasser [a], Francisco López Linares [b], Jean-François Lamonier [c], M. Josefina Pérez Zurita [a,*]

[a] *Universidad Central de Venezuela, Facultad de Ciencias, Escuela de Química, Centro de Catálisis, Petróleo y Petroquímica, Apartado Postal 40646, Los Chaguaramos 1040, Caracas,Venezuela*
[b] *Alberta Ingenuity Centre for In Situ Energy, CCIT Building, Chemical and Petroleum Engineering Department, University of Calgary, 2500 University Drive, NW Calgary, AB T2N 1N4, Canada*
[c] *Unité de Catalyse et de Chimie du Solide, UMR CNRS 8181, Université des Sciences et Technologies de Lille, 59650 Villeneuve d'Ascq, France*

Available online 22 November 2007

Abstract

The use of mesostructurated materials as cobalt support for the Fischer–Tropsch Synthesis (FTS) has taken increasing importance in the last decade. However, little use has been made of the hexagonal mesoporous silica (HMS), as most of the work has been reported for Co/MCM-41 and Co/SBA-15 catalytic systems. The effect of cobalt loading, impregnation method, particle size and pretreatment, on the catalytic properties of cobalt supported on HMS catalysts for the Fischer–Tropsch Synthesis have been studied. Catalysts were synthesized by incipient wetness impregnation, using an aqueous solution of hexahydrated cobalt nitrate as precursor salt. Additionally, a series of catalysts was prepared using an ethylene diamine cobalt complex which enabled cobalt nanoparticles formation. All catalysts were characterized by X-ray diffraction (XRD), temperature programmed reduction (TPR), chemical analysis and nitrogen adsorption. Calcination pretreatment has great influence in the catalytic behavior of the cobalt catalysts. All the catalysts prepared showed high C_5^+ fraction selectivity, specifically towards the diesel fraction. The use of HMS as cobalt catalyst support for the Fischer–Tropsch Synthesis seems to be very promising. When SiO_2 is used as support, C_5^+ hydrocarbons distribution shows a marked tendency towards C_{19}^+ fraction, while when HMS is used, the diesel fraction is favored. This result leads to the conclusion that the HMS pore structure produced a chain growth hindrance, tailoring the product distribution towards the diesel fraction.

Keywords: Fischer–Tropsch Synthesis; Cobalt; HMS; Diesel

1. Introduction

Climate change and air quality are major environmental concerns because they directly affect the way we live and breath. In order to meet the present and future threats generated by emissions to the atmosphere, environmental agencies around the world have issued more stringent regulations. One of them is the control of residual sulfur in diesel fuel and emission standards for particulates from diesel vehicles. All these facts have recently aroused renewed interest in the Fischer–Tropsch Synthesis because it can produce super clean diesel oil fraction with high cetane number (typically above 70) without any sulfur and aromatic compounds, using syngas from natural gas. Other factors such as the increase in the known reserves of natural gas, the need to monetize remote or stranded natural gas, environmental pressure to minimize flaring of associated gas and the improvements in the cost-effectiveness of the Fischer–Tropsch technology, boosted by the elevated oil prices, have contributed to this renewed interest in the use of Fischer–Tropsch technology for the conversion of natural gas to liquids [1–3]. Fischer–Tropsch Synthesis is catalyzed by transition metals, especially Co, Fe and Ru. Among them, cobalt-based catalysts are preferred for their high activity compared to Fe catalysts, high yields of long-chain paraffins, low activity for the competing water gas shift reaction (WGSR) and lower price than noble metals such as Ru [2,4,5].

* Corresponding author. Tel.: +58 212 605 1231; fax: +58 212 605 1220.
E-mail address: marperez@ciens.ucv.ve (M.J. Pérez Zurita).

1381-1169/$ – see front matter © 2007 Elsevier B.V. All rights reserved.
doi:10.1016/j.molcata.2007.11.014

One important issue in the development of high active cobalt catalysts for Fischer–Tropsch Synthesis is its improvement by increasing the number of active cobalt metal sites that are stable under reaction conditions. This is normally achieved by dispersing cobalt clusters on high area supports such as SiO_2, TiO_2 or Al_2O_3. Jacobs et al [6] reported that the choice of support not only largely determine the number of active sites stabilized after reduction, but it also influenced the amount of cobalt oxide species that can be reduced. Their temperature programmed reduction (TPR) and H_2 chemisorption with pulse reoxidation results show that the different supports did not stabilize a similar cluster size, and that the interaction between cobalt surface species and the support increased greatly for supports that stabilized smaller clusters (TiO_2 and Al_2O_3). The support porous structure could also affect cobalt dispersion, reducibility and FT catalytic behavior [7–9]. Khodakov et al. [7,8] have shown that in supported cobalt catalyst (5%), both the size of supported Co_3O_4 crystallites and their reducibility strongly depended on the pore size diameter of periodic mesoporous silica. Their catalytic experiments also showed that larger cobalt particles located in the wider silica pores were more active in Fischer–Tropsch Synthesis and produced lower methane selectivity than smaller cobalt particles located in narrower pore supports. Faujasite zeolites have also been used as cobalt support for Fischer–Tropsch Synthesis catalysts. Wang et al. [10] synthesized metallic cobalt nanoparticles in faujasite zeolites by reducing Co_2^+-exchanged zeolites with sodium borohydride aqueous solutions. They claimed that Co particles with a maximum size distribution of 1–2 nm, which are probably located inside the supercages of faujasite zeolites, can be obtained and exhibited higher CO conversions in Fischer–Tropsch Synthesis than larger cobalt particles located outside the supercage or on the surface of a nonporous silica.

The use of mesostructurated materials as cobalt support for Fischer–Tropsch Synthesis has taken increasing importance in the last decade [1,2,7–9,11–13]. Ohtsuka et al. [12] examined the effect of the average pore diameter (from 3.5 to 13 nm) of Co/SBA-15 catalysts on the Fischer–Tropsch Synthesis performance, and found that the catalyst with pore diameter around 8 nm showed the largest conversion. This result was explained by the interplay between catalyst reducibility and dispersion. The influence of cobalt loading and cobalt precursor on the physical–chemical and catalytic properties of cobalt-based catalysts supported on mesoporous materials for the Fischer–Tropsch Synthesis have also been investigated. Martinez et al. [2] studied the loading effect of cobalt (10–40%, w/w) supported on SBA-15 and showed that the maximum CO conversion was obtained for a catalyst loaded with 30 wt% Co which presented the highest density of surface cobalt sites. However, the intrinsic activity of cobalt remained constant in the range of cobalt loading studied. Their product selectivity was also influenced by cobalt loading. The formation of C_5^+ hydrocarbons was favored over catalysts presenting high reducibility. Most of the cobalt species in the catalysts prepared from organic cobalt precursors were strongly interacting with the support, which led to very low Fischer–Tropsch Synthesis activities and high methane selectivity.

Little use [14] has been made of the HMS as support for Fischer–Tropsch Synthesis cobalt catalysts. HMS mesoporous silica was first introduced by Pinnavaia and co-workers [15,16]. As compared to MCM-41 and SBA-15, HMS is less ordered showing a wormhole-like pore structure and monodispersed pore diameter, thick pore walls and a high degree of condensation; therefore, high thermal stability. In addition, the mesopores on HMS are shorter, allowing faster diffusion of reactants. Yin et al. [14] reported on the catalytic properties for Fischer–Tropsch Synthesis of HMS and MCM-41. The Co/HMS catalyst showed better catalytic activity and C_5^+ selectivity. Their results were explained in term of the narrower pore size distribution with shorter channels and larger textural mesoporosity of the HMS mesoporous silica. With increasing cobalt loading on the HMS support, the reduction temperature of cobalt oxides slightly increases, but the activity also increases, caused by the presence of more active sites in the channels of HMS.

In the present work, we have studied the catalytic behavior of cobalt-supported on the HMS mesoporous material for the Fischer–Tropsch Synthesis. The influence of cobalt loading, cobalt precursor salt and pretreatment conditions on the physical–chemical and catalytic properties of Co/HMS catalysts were investigated.

2. Experimental

2.1. Preparation of catalysts

The synthesis of the HMS support was carried out using the procedure described by Tuel [17]. In a typical synthesis a homogeneous mixture comprising 11.15 mL of tetraethyl orthosilicate (TEOS), 8.71 mL of ethanol (EtOH) and 3.83 mL of *iso*-propanol (iPrOH) was added to a homogeneously stirred solution of 3.62 g of $CH_3(CH_2)_{15}NH_2$, 9.0 mL of EtOH and 32.4 g of distilled water. The resultant gel (molar composition 0.05 TEOS: 0.3 EtOH: 0.05 iPrOH: 0.015 $C_{16}H_{35}N$: 1.8 H_2O) was maintained under stirring for 2 h. After this time, the mixture was kept at rest for 24 h. All the synthesis procedure was performed at room temperature. The as-synthesized HMS was separated by centrifugation, washed with ethanol under reflux for 2 h, dried at room temperature and finally calcined in air flow at 773 K for 6 h to remove the organic template.

Two series of catalysts were prepared using HMS as support. The first series was prepared by incipient wetness impregnation, using an aqueous solution of hexahydrated cobalt (II) nitrate (Alpha, 98.9% purity) as precursor salt. This series is referred as *X*Co(N)*T*/HMS, where *X* represents the nominal cobalt content, N stands for nitrate and *T* indicates the calcination temperature. The second series was prepared using a new and simple method for obtaining highly dispersed Co catalyst reported by Wyrwalski et al. [18]. The reason why ethylene diamine improves dispersion of the cobalt species was explained in terms of the size of the stable complex ions which were formed in situ during impregnation: as the cobalt atom is surrounded by the ethylene diamine ligands, they are forced to be far apart one from another leading to highly dispersed catalyst.

This series was prepared by impregnation using a solution of cobalt (II) nitrate and ethylene diamine (Co/ethylene diamine molar ratio of 1) dissolved in excess water with respect to the pore volume of the HMS support (liquid/solid ratio of 50 cm^3/g), followed by slow evaporation of the solvent in a rotary evaporator at 333 K and vacuum until dryness. Catalysts of this series are referred as *X*Co(en)*T*/HMS, where *X* represents the nominal cobalt content, en stands for ethylene diamine and *T* indicates the calcination temperature. For comparison purposes, two Co/SiO_2 catalysts (one for each series) were also prepared, incorporating the cobalt by the same procedure described for them. A commercial amorphous silica (Davinson Grade 69, $d_p = 12$ nm, $V_p = 1.4$ mL/g, $S_{BET} = 340$ m^2/g, PV = 0.81 cm^3/g) was used as support.

2.2. Characterization techniques

Catalysts composition was determined by atomic absorption using a GBC Avanta equipment. Nitrogen isotherms at 77 K were measured using a Micromeritics TriStar 3000 apparatus. Prior to the adsorption measurements, the samples were out gassed overnight at 523 K. Nitrogen isotherms were obtained in both adsorption and desorption modes. The surface areas of supports and catalysts were determined by the BET method. The total pore volume was calculated from the amount of vapor adsorbed at a relative pressure (P/P_o) close to unity, where P and P_o are the measured and equilibrium pressures, respectively. Pore size distribution was established from the adsorption branches of the isotherms using the Barrett–Joyner–Halenda (BJH) method.

X-ray diffraction patterns were obtained at room temperature in a Phillips D8 AVANCE diffractometer model PW1830 using a Ni-filtered Cu Kα radiation (40 kV, 25 mA). The sweeping used for all the samples was from 10° to 70° 2θ at a rate of 2°/min. The Co_3O_4 average particle size was calculated using the Scherrer equation $d = (k\lambda/(B\cos\theta))(180^\circ/\pi)$ for the more intense peak ($2\theta = 36.8^\circ$) where d is the average crystal particle diameter, k is the Scherrer constant (0.89), λ is the used wave length (1.54056 Å for Cu) and B is the peak width at the middle height in degrees.

In order to examine the reducibility of the cobalt species in the calcined catalyst, temperature programmed reduction profiles were obtained in a ThermoQuest 1100 equipment of CE instrument. A sample of about 100 mg was placed in a quartz tubular reactor, using a flow of 20 mL/min of a 10% H_2 in argon mixture with a heating rate of 10 °C/min from room temperature to 1323 K.

2.3. Catalytic tests

The Fischer–Tropsch Synthesis reaction was performed in a down-flow fixed-bed stainless-steel reactor ($d_i = 10$ mm, $l = 30$ cm). The reactor was loaded with 0.30 g of catalyst. Prior to the catalytic experiments, the catalysts were reduced in situ at atmospheric pressure by increasing the temperature at 2 K/min. Standard reduction conditions for conventional cobalt supported catalyst are 673 K and a reduction time of around 4 h. However, these conditions could vary depending on the Co–support interactions. In the present study, the reduction temperature used for each series was determined from the TPR experiments. For the N-series, the reduction temperature was 673 K and it was kept for 12 h, while for en-series the temperature of reduction was 973 K and was maintained for 10 h. After the reduction step, the temperature was lowered to 463 K under H_2 and the reactant gas mixture (H_2:CO:N_2, 63:32:5, v/v, N_2 as internal standard) was introduced at a total flow rate of 30 L/min (GHSV of 5.4 L(NTP)/(g_{cat} h), increasing the system pressure slowly up to 20 bar. Temperature in the catalyst bed was increased afterwards from 463 K to 503 K at a controlled heating rate of 2 K/min. Once the reaction temperature was achieved, the reaction was led to proceed during a period of 120 h.

During reaction, the reactor effluent passed through a hot trap kept at 423 K and 20 bar to collect waxes, and the products leaving this trap were passed through a second trap kept at 273 K and 20 bar to collect the lighter products (water, alcohols and hydrocarbons). The effluent gases were depressurized and analyzed periodically by on-line gas chromatography. The analyses were performed in various chromatographs according to the nature of the sample to be analyzed. Permanent gases and light hydrocarbons were analyzed in line in a PerkinElmer 3000GC Autosystem fitted with TCD and FID detectors using a Carbosieve SII Supelco column and an Alumina RT column, respectively. The liquid products (collected at 423 K and 273 K) were weighted and analyzed using two chromatographs. The liquid hydrocarbons were analyzed in a Varian 3300 fitted with a 30 m long Supelco Alumina KCl capillary column connected to a FID. The aqueous products were analyzed in a Varian series 3300 with a Porapack Q column connected to TCD.

3. Results and discussion

3.1. Chemical analysis and textural properties

Table 1 shows the cobalt content and textural properties of the studied catalysts. Nominal and real cobalt contents were very similar. Cobalt introduction leads to a sharp decrease in specific surface area in all cases, being more pronounced for N-series catalysts. This result could suggest that particle size in this series is larger. However, loss of surface area could be explained by several factors, none of them been the unique cause. Beside partial blockage of pores, the impact of impregnation on the ordered structure of mesoporous supports could be high. Khodakov et al. [11] reported for MCM-41, that aqueous impregnation followed by drying, leads to loss of long range ordering and to a substantial decrease in surface area and pore volume. However, for the SBA-15 they found that the structure remains almost intact after introduction of significant amounts of cobalt. The different behavior of these two mesoporous silica materials was mainly attributed to their different pore wall thickness. Our results seem to be consistent with this fact as the wall thickness of the HMS synthesized in the present study (~3 nm, not shown) is larger than that reported for MCM-41 (~1.7 nm) but thinner than that of SBA-15 (~5.4 nm). On the other hand, part of the decrease in the surface area could also be related to the "dilution" of the siliceous support with cobalt oxide. Average pore diame-

Table 1
Chemical composition and textural properties obtained from N_2 adsorption isotherms of HMS-supported cobalt catalysts

N-series					En-series				
Catalyst	Co (wt%)	S_{BET} (m^2/g)	AVDp (nm)	Total pore volume (cm^3/g)	Catalyst	Co (wt%)	S_{BET} (m^2/g)	AVDp (nm)	Total pore volume (cm^3/g)
10Co(N)400/HMS	8.9	314	7.2	0.5809	10Co(en)400/HMS	10.3	420	6.4	0.6983
20Co(N)400/HMS	26	369	6.3	0.6215	20Co(en)400/HMS	22.3	371	6.3	0.6170
10Co(N)400/SiO_2	10.3	297	–	–	20Co(en)400/SiO_2	19.9	322	–	–
HMS	–	805	6.0	1.2064	SiO_2	–	340	12.0	1.400

ter (AVDp) values are similar to those reported in the literature [14].

3.2. X-ray diffraction results

To determine the cobalt species present in the different catalysts, their average particle sizes estimated from the Scherrer equation, the *d*-spacing from the (1 0 0) reflection peak and the unit cell parameter were determined by X-ray diffraction (XRD) of the support and the calcined catalysts. Some differences can be observed among the studied series. Fig. 1 shows the XRD patterns of catalysts from en-series. While catalyst 10Co(en)/HMS shows no distinct signals, catalyst 20Co(en)/HMS shows five sharp signals characteristic of Co_3O_4 spinel (PDFWIN 42-1467). In contrast, for all catalysts of N-series (Fig. 2) cobalt is present in the form of the Co_3O_4 spinel and its five characteristic signals can be clearly identified. When increasing the cobalt content, the peaks become narrower, indicating an increase of Co_3O_4 mean particle size. The fact that no distinct signals are visible in the catalyst 10Co(en)/HMS seems to indicate that, in this sample, cobalt should be highly dispersed on the HMS surface. Similar results were reported by Martinez et al. [2] for Co(16%)/SBA-15 prepared from Co-acetylacetonate, Sun et al. [19] for Co(10%)/SiO_2 and Wang et al. [20] for Co(20%)/SBA-15 both prepared from cobalt acetate. In all these cases, the absence of diffraction signals was taken as evidence of highly dispersed cobalt species as a consequence of the presence of nanosized Co_3O_4 clusters in the surface of the support. Nevertheless, the absence of Co_3O_4 reflections in supported Co catalysts, especially on siliceous materials and on Al_2O_3, does not necessarily imply the presence of very small Co_3O_4 particles, but could also be due to amorphous cobalt silicates formation induced by strong cobalt–support interactions. Yin et al. [14], in their Co(15%)/HMS catalyst prepared from cobalt nitrate, could not detect any XRD signal with cobalt contents as high as 15% (w/w). In their work, no chemical analyses results were reported, so probably the real cobalt content in their catalysts was lower than the nominal content. The average crystal size of the oxidized form of cobalt for all the studied catalysts is show in Table 2. As expected, particle sizes for en-series catalysts were smaller than those of N-series catalysts. This observation suggests that cobalt species are highly dispersed in the former series.

In order to study the effect of calcination temperature on cobalt–support interaction, 20Co(N)/HMS catalyst was calcined at 473, 573 and 673 K. Fig. 3 shows the diffraction patterns for these catalysts and Table 3 shows the average particle size calculated from Scherrer equation. As the calcination temperature increases, the average particle size slightly increases. Although

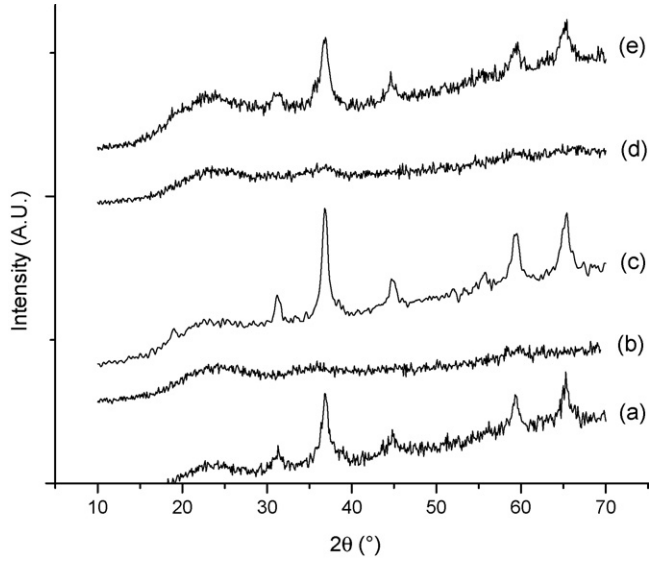

Fig. 1. XRD patterns of (a) 20Co(en)/SiO_2, (b) 10Co(en)/HMS, (c) 20Co(en)/HMS, (d) 10Co(en)550/HMS and (e) 10Co(en)/HMS directly reduced and re-oxidized after reduction.

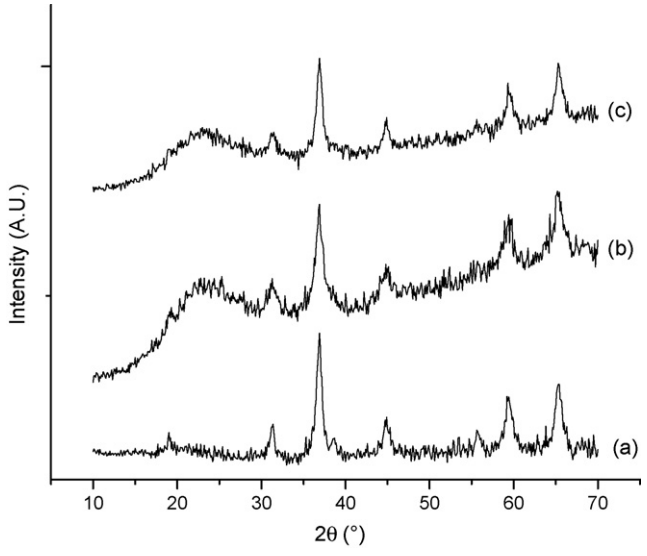

Fig. 2. XRD patterns of (a) 10Co(N)/SiO_2, (b) 10Co(N)/HMS and (c) 20Co(N)/HMS.

Table 2
XRD results: average particle size

N-series		En-series	
Catalyst	Average particle size[a] (nm)	Catalyst	Average particle size[a] (nm)
10Co(N)400/HMS	15	10Co(en)400/HMS	nd
20Co(N)400/HMS	16	20Co(en)400/HMS	10
10Co(N)400/SiO_2	16	20Co(en)400/SiO_2	10
HMS	–	SiO_2	–

nd = not detected.
[a] Calculated from the Scherrer equation.

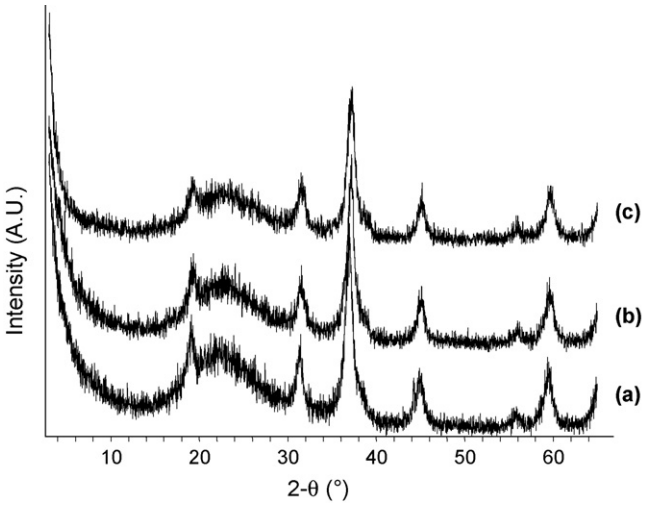

Fig. 3. XRD patterns of (a) 20Co(N)200/SiO_2, (b) 20Co(N)300/SiO_2 and (c) 20Co(N)400/SiO_2.

it is expected that cobalt–support interaction increases with calcination temperature and sintering diminishes, in the studied range of temperature it seems that the interaction is not strong enough as to avoid particle growing due to sintering. This observation, although not conclusive as the increase of the particle size observed was marginal, shows a tendency which have to be studied with more details. Increasing calcination temperature to 10Co(en)/HMS catalyst from 673 K to 823 K (Fig. 1) did not have the same effect as no changes in the diffraction pattern were observed. A stronger cobalt interaction with the support for en-series catalysts could explain this result. With the aim of studying the Co–support interaction without previous calcination, the 10Co(en)/HMS catalyst was directly reduced at 973 K and reoxidized under mild conditions (523 K for 3 h) for subsequent analysis by XRD. A distinct XRD pattern was obtained (Fig. 1b) and the calculated particle size was 8 nm. In this case, it is evident that weak or no interaction exist and that the pretreatment used to activate the catalyst strongly affect the interaction between cobalt and support.

Table 3
Effect of calcination temperature on the average particle size for catalyst 10Co(N)/HMS

Catalyst	Average particle size[a] (nm)
20Co(N)200/HMS	13
20Co(N)300/HMS	14
20Co(N)400/HMS	16
10Co(en)NC[b]/HMS	8[c]

[a] Calculated from the Scherrer equation.
[b] NC = not calcined.
[c] Re-oxidized after reduction.

3.3. Temperature programmed reduction

It is often desirable to know the precise conditions under which a precursor will become reduced to an active form, and whether the process is a simple or a complex one, that is to say, whether the reduction takes place in one stage or if it is a stepwise reduction with species of different degree of reducibility. A widely used technique for answering these questions is the temperature programmed reduction. By far, the greatest use made of TPR is, in a finger-printing sense, to recognize the number and type of precursor species and their reducibility.

It has been widely reported that the reduction of supported Co_3O_4 takes place in two stages: a first one assigned to the reduction of Co_3O_4 to CoO, followed by the subsequent reduction of CoO to Co [2,6,14,21,22]. Fig. 4 shows the TPR profiles of en-series catalysts. All catalysts supported on HMS mesoporous silica in this series show a very poor reducibility reflected by the high temperatures at which they are reduced. The catalyst with the lowest Co content supported on HMS (Fig. 4b) showed a small and broad reduction peak at around 580 K and a more intense one at 820 K. This result corroborates the XRD observations suggesting a strong Co–support interaction as a consequence of the presence of very small particles in this catalyst. The same catalyst calcined at a higher temperature (823 K, Fig. 4d) also showed two broad bands at around 650 K and 1100 K. Calcination at higher temperature increases the cobalt–support interaction making the solid less reducible. When the Co loading increases (Fig. 4c), a third peak appears at around 700 K and the low temperature signal is more intense and shifts to a lower value (∼500 K) meaning that the sample

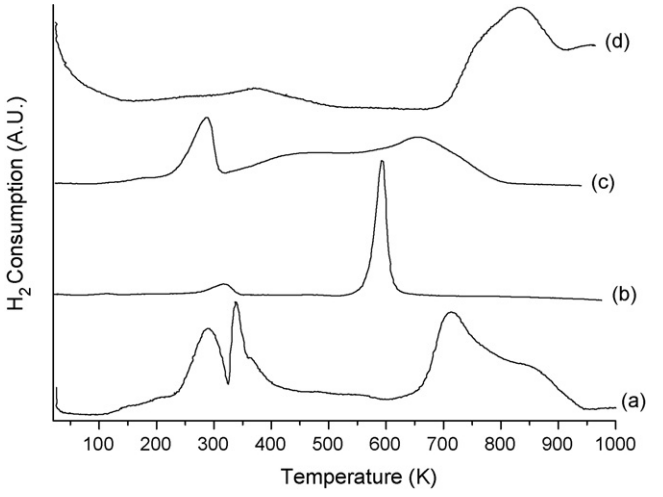

Fig. 4. TPR profiles of (a) 20Co(en)/SiO_2, (b) 10Co(en)/HMS, (c) 20Co(en)/HMS and (d) 10Co(en)550/HMS.

Table 4
Temperature programmed reduction results: hydrogen consumption and reducibility of the studied catalysts

N-series			En-series		
Catalyst	Total hydrogen consumption[a] (μmol/g_{cat})	Reducibility[b] (%)	Catalyst	Total hydrogen consumption[a] (μmol/g_{cat})	Reducibility[b] (%)
10Co(N)400/HMS	1909	100	10Co(en)400/HMS	2076	89
20Co(N)400/HMS	5213	90	20Co(en)400/HMS	4503	89
20Co(N)200/HMS	5800	100	20Co(en)400/SiO_2	4323	96
10Co(N)400/SiO_2	2567	100	10Co(en)550/HMS	1479	63

[a] Calculated between RT and 1200 K.
[b] Reducibility was defined as (μmol H_2 consumed/g_{cat})$_{experimental}$/(μmol H_2 consumed/g_{cat})$_{theoretical}$.

reduces more easily. Again, these results are in line with the XRD results. The coexistence of Co_3O_4 spinel species, which reduces at lower temperature, with Co species strongly interacting with the support, seems evident.

For SiO_2 supported catalyst (Fig. 4a), two well-defined doublets were observed with T_{max} at around 550–650 K and 980–1100 K. In this case, the expected doublet assigned to the two stages reduction of Co_3O_4 is observed. It is evident that reducibility of this catalyst is higher than that observed when HMS mesoporous silica is used as support. The presence of a second doublet at higher temperature has already been reported by Martinez et al. [2] who assigned the doublet to the presence of surface Co species with a higher interaction with the support, possibly cobalt silicates species formed during TPR experiments by reaction of highly dispersed CoO with the siliceous material. However, this assignment is not straight forward since either explanation, Co silicate or Co_3O_4 small particles with high interaction with the support would produce similar TPR profiles. The reducibility values obtained (Table 4) are in complete agreement with the XRD results discussed above: as the particle size is diminished, reducibility is low. As expected, N-series catalysts, Fig. 5 and Table 4, reduces to a larger extent and at much lower temperatures (T_{max}, 480–980 K). For this series, the catalysts supported on HMS showed two doublets ascribed, as for 20Co(en)400/SiO_2, to two different Co species. When the support was SiO_2 (Fig. 5a), the reducibility is higher and only a very small signal was observed at higher temperature. For both series the results seem to indicate that cobalt interaction with HMS is stronger than the interaction with the SiO_2 support.

Fig. 6 shows the TPR profiles for 20Co(N)/HMS catalyst calcined at different temperatures. Again the results are in complete agreement with XRD observations: as the calcination temperature increases, for N-series catalysts, the reducibility is higher in accordance with larger particle sizes. Table 4 shows the total hydrogen consumption and the degree of reduction for the studied series. It is observed that the N-series reduce in a higher extent that the en-series, in agreement with the T_{max} discussion made above. Again, reducibility of the cobalt species present in the catalyst with the lowest cobalt content reduced at a higher temperature (10Co(en)550/HMS) was very low. This result is not expected as even cobalt silicates reduce at the maximum temperature used in the study. The presence of very small CoO particles stabilized by the HMS support could explain this result.

3.4. Catalytic results

The results of syngas conversion, product distribution and chain growth probability (α) are shown in Table 5. N-series catalysts are more active than those from en-series. In principle, a correlation of activity with the reducibility obtained from the TPR measurements and the particle size obtained from XRD

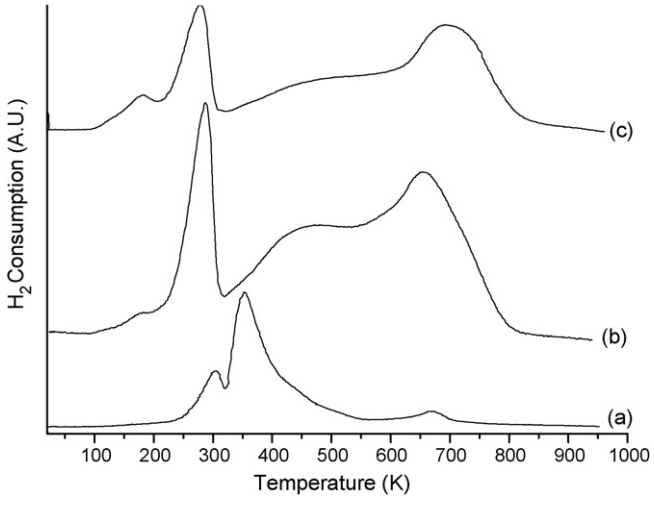

Fig. 5. TPR profiles of (a) 10Co(N)/SiO_2, (b) 10Co(N)/HMS and (c) 20Co(N)/HMS.

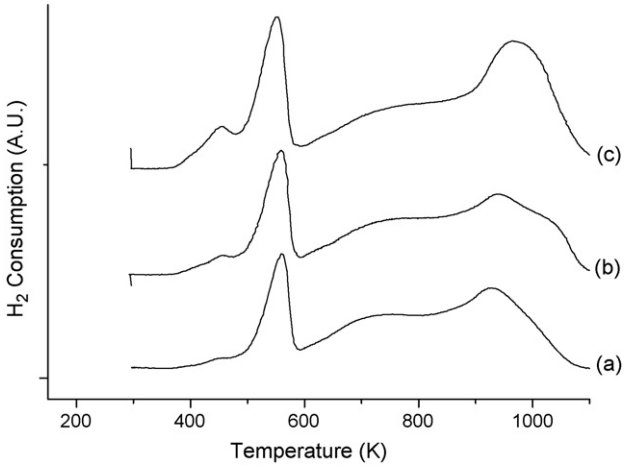

Fig. 6. TPR profiles of (a) 20Co(N)400/HMS, (b) 20Co(N)300/HMS and (c) 20Co(N)200/HMS.

Table 5
Catalytic activity and selectivity on Fischer–Tropsch Synthesis

N-series							En-series						
Catalyst	XCO (%)	Selectivity (%)					Catalyst	XCO (%)	Selectivity (%)				
		CO_2	CH_4	C_2–C_4	C_5^+	α			CO_2	CH_4	C_2–C_4	C_5^+	α
10Co(N)400/HMS	16	0.0	17.5	27.3	54.3	0.74	10Co(en)400/HMS	10	1.0	38.4	20.4	39.0	0.74
20Co(N)400/HMS	23	2.4	19.0	11.4	65.9	0.77	20Co(en)400/HMS	12	0.0	35.4	22.1	41.7	0.82
20Co(N)200/HMS	21	3.0	28.1	17.1	50.6	0.80	20Co(en)400/SiO_2	13	1.4	22.2	30.7	44.8	0.86
10Co(N)400/SiO_2	25	0.0	8.2	12.6	78.6	0.86							

results can be established. The potential benefit of a better dispersion cannot be observed for the en-series catalysts probably because of their poor reducibility. This result is not surprising as the dispersion–reducibility dependence inherent to very small cobalt particles, supported on siliceous material, is very well documented. Very recently Martínez and Prieto [23] reported on a methodological preparation approach which they claim allows breaking this dependence using cobalt nanoparticles synthesized in a reverse microemulsion, supported on a surface protected delaminated ITQ-2 zeolite. Conversion seems to be little affected when increasing cobalt content or changing support and calcinations temperature for en-series catalysts. It is not the case for the N-series catalysts where the expected increase of conversion with cobalt content was observed. Also for this series, changing HMS for SiO_2 support leads to an increase in conversion which could be explained in terms of the higher cobalt content and higher particle size of the 10Co(N)400/SiO_2 catalyst.

Several differences can be observed in the product distribution when changing the preparation method, cobalt content, particle size and support. N-series catalysts are less selective towards methanation while their selectivity towards the C_5^+ fraction is high. This result is ascribed to the larger particle size of the cobalt species present in this series. Increasing the cobalt content did not affect the product distribution in the same way. For N-series catalysts, C_5^+ fraction selectivity increases at the expenses of the C_2–C_4 fraction while for en-series, no change in the product distribution was observed. The fact that chain growth seems to be different for both series suggest different chain growth mechanism. As chain growth in N-series seems to be related to the C_2–C_4 fraction, the mechanism involved could be light olefin re-adsorption while a conventional Anderson Shultz Flory mechanism could be invoked to explain chain growth on en-series. Support effect is also more marked in N-series although the trend is similar. In this case, for both series, the use of a conventional SiO_2 support lead to a product distribution similar to that obtained for en-series, C_5^+ fraction selectivity increases at the expenses of the CH_4.

When a lower calcinations temperature is used (20Co(N)200/HMS catalyst) C_5^+ fraction selectivity decreases at the expenses of the CH_4. A possible explanation for this result was given by Reuel and Batholomew [24]. These authors attributed a high selectivity towards methane formation to the presence of unreduced cobalt oxide species, which are active towards the WGSR. If this reaction takes place, the effective H_2/CO ratio increases on the catalyst surface therefore favoring

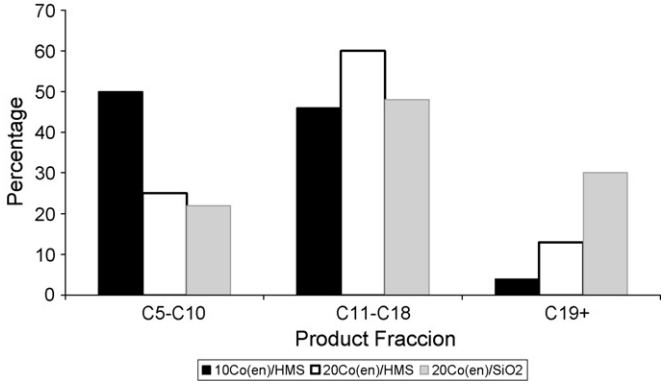

Fig. 7. Higher hydrocarbon distribution for en-series.

the hydrogenation of adsorbed species and methane selectivity. This observation seems to be satisfactory for this particular case as the selectivity towards CO_2 was the highest for this catalyst. When no previous calcination was used, a sharp and very rapid deactivation took place implying a weak cobalt support interaction which leads to metal sintering. A very low CO_2 selectivity is observed for both series, which is consistent with the low activity of cobalt to catalyze the water gas shift reaction. No significant amounts of oxygenated products (<1%) were obtained in all the studied catalysts.

Figs. 7 and 8 show the higher hydrocarbon distribution for the catalysts of en-series and N-series, respectively. Catalysts from both series were more selective towards the diesel fraction (C_{11}–C_{18}). Cobalt content in en-series has a marked effect on product distribution. While 10Co(en)400/HMS cata-

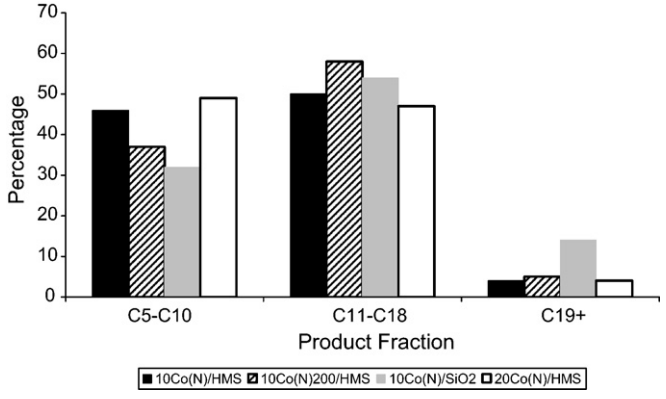

Fig. 8. Higher hydrocarbon distribution for N-series.

lyst was more selective towards the gasoline fraction (C_5–C_{10}), 20Co(en)400/HMS catalyst was more selective towards the diesel fraction. Again, it is possible as discussed above, that the unreduced cobalt species, produce a higher H_2/CO ratio on the surface of the catalyst leading to chain termination and to a lower chain growth probability for 10Co(en)400/HMS catalyst.

In N-series catalysts, the cobalt content does not have an important effect on the hydrocarbon distribution, however, shape selectivity due to the pore structure of HMS is once again observed. Many studies of Fischer–Tropsch Synthesis have suggested that the pore size of support could significantly affect the Fischer–Tropsch Synthesis reaction rate and hydrocarbon selectivity. Okabe et al. [25] reported that wide pore catalysts are preferable for higher conversion and higher C_5^+ selectivity because of the higher reducibility of large cobalt particles in wide pores over the pore size range from 4 to 10 nm. Ohtsuka et al. [12] prepared cobalt catalysts supported on SBA 15 with different pore diameters using ethanol solution of cobalt acetate. They found that the catalyst with moderate pore diameter of 8.3 nm provided the highest CO conversion. Saib et al. [26] also reported that the catalyst supported on silica with average pore diameter of 10 nm was the most active and selective for hydrocarbon formation in Fischer–Tropsch Synthesis. C_5^+ and methane selectivity passed through a maximum and a minimum, respectively at the 10 nm supported catalyst. Song and Li [27] reported that support effects on product selectivity are more complicated than on activity. Their results also show that the porosity of the silica support affect not only the cobalt particle size but also the product distribution, their C_5^+ selectivity passes through a maximum with increasing pore size and reaches its peak value at 7 nm while the reverse trend was observed for CH_4 selectivity. Moreover, some authors [28,29] considered that carbon monoxide diffusion limitation in the pores of catalysts could increase H_2/CO ratio and thus increase the methane selectivity. Our results seem to point out to a possible restriction effect exerted by the HMS pore structure. However, more experiments have to be made in order to rule out other possible explanation.

4. Conclusions

The use of HMS as cobalt catalysts support for the Fischer–Tropsch Synthesis seems to be very promising. When SiO_2 is used as support, the product distribution among the C_5^+ hydrocarbons shows a marked tendency towards the C_{19}^+ fraction, while on HMS, the diesel fraction is favored. It is possible that the HMS pore structure hinders hydrocarbon chain growth by exerting a restriction effect on the chain growth which would tailor the product distribution towards the diesel fraction. The calcination pretreatment have great influence in the catalytic behavior of the cobalt catalysts. The catalysts prepared using an ethylene diamine cobalt complex, were better dispersed, showing smaller particle sizes which were less reducible, leading to a lower catalytic activity towards the Fischer–Tropsch Synthesis. Finally, no significant amounts of oxygenated products were obtained in all the studied catalysts (<1%).

Acknowledgements

The authors would like to acknowledge the financial support of FONACIT through Project No. S1-2000000530.

References

[1] Y. Ohtsuka, T. Arai, S. Takasaki, N. Tsubouchi, Energy Fuels 17 (2003) 805.
[2] A. Martinez, C. Lopez, F. Marquez, I.J. Diaz, Catalysis 220 (2003) 486.
[3] J.M. Girardon, A. Constant-Griboval, L. Gengembre, P.A. Chernavskii, A.Y. Khodakov, Catal. Today 106 (2005) 161.
[4] P. Chaumette, P. Courty, A. Kiennemann, B. Ernst, Top. Catal. 2 (1995) 117.
[5] J.G. Googwin Jr., ACS Prepr. Symp. 36 (1) (1991) 156.
[6] G. Jacobs, T.K. Das, Y. Zhang, J. Li, G. Racoillet, B.H. Davis, Appl. Catal. A: Gen. 233 (2002) 263.
[7] R. Bechara, D. Balloy, D. Vanhove, Appl. Catal. A: Gen. 207 (2001) 343.
[8] A.Y. Khodakov, R. Bechara y, A. Griboval-Constant, Appl. Catal. A: Gen. 254 (2003) 273.
[9] A.Y. Khodakov, A. Griboval-Constant, R. Bechara, V.L. Zholobenko, J. Catal. 206 (2002) 230.
[10] Y. Wang, H. Wu, Q. Zhang, Q. Tang, Micropor. Mesopor. Mater. 86 (2005) 38.
[11] A.Y. Khodakov, V.L. Zholobenko, R. Bechara, D. Durand, Micropor. Mesopor. Mater. 79 (2005) 29–39.
[12] Y. Ohtsuka, Y. Takahashi, M. Noguchi, T. Arai, S. Takasaki, N. Tsubouchi, Y. Wang, Catal. Today 89 (2004) 419.
[13] E. Iglesia, Appl. Catal. A: Gen. 161 (1997) 59.
[14] D. Yin, W. Li, W. Yang, H. Xiang, Y. Sun, B. Zhong, S. Peng, Micropor. Mesopor. Mater. 47 (2001) 15.
[15] P.T. Tanev, M. Chibwe, T.J. Pinnavaia, Nature 368 (1994) 321.
[16] P.T. Tanev, T.J. Pinnavaia, Science 167 (1995) 865.
[17] A. Tuel, Micropor. Mesopor. Mater. 27 (1999) 151.
[18] F. Wyrwalski, J.-F. Lamonier, M.J. Perez-Zurita, S. Siffert, A. Aboukais, Catal. Lett. 108 (1–2) (2006) 87.
[19] S. Sun, N. Tsubaki, K. Fujimoto, Appl. Catal. A 202 (2000) 121.
[20] Y. Wang, M. Noguchi, Y. Takahashi, Y. Ohtsuka, Catal. Today 68 (2001) 3.
[21] P. Concepción, C. López, A. Martínez, V.F. Puntes, J. Catal. 228 (2004) 321.
[22] G.R. Moradi, M.M. Basir, A. Taeb, A. Kiennemann, Catal. Commun. 4 (2003) 27.
[23] A. Martínez, G. Prieto, J. Catal. 245 (2007) 470.
[24] R.C. Reuel, C.H. Batholomew, J. Catal. 85 (1984) 78.
[25] K. Okabe, X.H. Li, M.D. Wei, H. Arakawa, Catal. Today 89 (2004) 431.
[26] A.M. Saib, M. Claeys, E.V. Steen, Catal. Today 71 (2002) 395.
[27] D. Song, J. Li, J. Mol. Catal. A: Chem. 247 (2006) 206.
[28] J.A. Lapszewicz, H.J. Loch, J.R. Chipperfield, J. Chem. Soc., Chem. Commun. (1993) 819.
[29] M. Kraum, M. Baerns, Appl. Catal. A: Gen. 186 (1999) 189.